arXiv:0806.0556v3 [hep-ph] 28 Oct 2009

A study on the anomaly of p over π ratios in $Au + Au$ collisions with jet quenching

Xiaofang Chen[1,2], **Hanzhong Zhang**[1,2,3], **Ben-Wei Zhang**[1,2] **and Enke Wang**[1,2]

[1]Institute of Particle Physics, Huazhong Normal University, Wuhan 430079, China
[2]Key Laboratory of Quark & Lepton Physics (Huzhong Normal University), Ministry of Education, China
[3]Department of Physics, Shandong University, Jinan 250100, China

Abstract. The ratios of p/π at large transverse momentum in central $Au + Au$ collisions at RHIC are studied in the framework of jet quenching based on a next-to-leading order pQCD parton model. It is shown that theoretical calculations with a gluon energy loss larger than the quark energy loss will naturally lead to a smaller p/π ratios at large transverse momentum in $Au+Au$ collisions than those in $p+p$ collisions at the same energy. Scenarios with equal energy losses for gluons and quarks and a strong jet conversion are both explored and it is demonstrated in both scenarios p/π ratios at high p_T in central $Au + Au$ collisions are enhanced and the calculated ratios of protons over pions approach to the experimental measurements. However, $\bar{p}/p$ in the latter scenario is found to fit data better than that in the former scenario.

PACS numbers: 12.38.Mh,24.85.+p,25.75.-q

1. Introduction

Relativistic heavy-ion collisions provide the possibility of creating in the laboratory a plasma of deconfined quarks and gluons, or QGP. So far a large amount of interesting data have been accumulated in the experiments at the Relativistic Heavy Ion Collider (RHIC) [1, 2, 3, 4], which strongly suggest a new kind of matter may have been formed at RHIC. One of the most striking evidences of the formation of QGP is the strong suppression of hadron spectra with large transverse momentum (or high p_T) in $Au + Au$ collisions as compared to $p + p$ collisions [5, 6]. This kind of suppression agrees with the prediction of jet quenching theory [7, 8, 9, 10, 11], which has provided compelling explanations on many novel phenomena at high p_T observed at RHIC, such as the suppression of π^0 production at high p_T, and the disappearance of back-to-back correlations of high p_T hadrons [12].

In the picture of jet quenching or parton energy loss, an energetic parton will loss energy by multiple scattering in the medium when it propagates through the hot QGP medium. The majority of current approaches to the medium-induced parton energy loss may be divided into four major schemes which included higher twist(HT) [13, 14, 15, 16], path integral approach to the opacity expansion (BDMPS-Z/ASW) [17, 18, 19, 20], finite temperature field theory approach(AMY) [21, 22, 23] and reaction operator approach to the opacity expansion (GLV) [24, 25, 26, 27]. It has been shown that the energy loss of light quarks and gluons is proportional to the gluon density and has a quadratic dependence on the total distance traversed by the propagating parton due to the non-Abelian LPM interference effect in multiple scatterings [18, 24, 28, 29, 30]. Moreover it is expected that the gluon energy loss in nuclei is 9/4 times of the quark energy loss due to the different color factors for quark-gluon vertex and gluon-gluon vertex [7, 29, 30]. Because high p_T proton (anti-proton) production in $p + p$ collisions is dominated by gluon fragmentation whereas high p_T pion at $p + p$ collisions is dominated by quark fragmentation, it is expected that larger gluon energy loss than quark energy loss in hot/dense medium will lead to a smaller p/π ratio at high p_T in $Au + Au$ collisions than in $p + p$ collisions at the same energy [31].

However, STAR Collaboration recently published very interesting measurements which indicate that p/π^+ and $\bar{p}/\pi^-$ ratios at high p_T in central Au+Au collisions [32] approach those in $p + p$ and $d + Au$ collisions [33], and the nuclear modification factor of protons is similar to that of pions [32]. To solve the discrepancy between the experimental data and the theoretical calculations, a jet conversion mechanism [34] has been proposed by taking into account the possibility of a quark jet in QGP converted into a gluon jet and vice versa, which has previously been considered theoretically in Refs. [35] for eA deeply inelastic scattering within higher twist expansion approach. It is found that conversions between quark and gluon jets indeed lead to an increase in the final number of gluon jets in central heavy ion collisions than the case without conversions, but to explain experimental data observed by STAR a conversion enhancement factor $K = 4 \sim 6$ would be needed [34].

In this paper, we will study the p/π ratio in $Au+Au$ collisions with $\sqrt{s} = 200$ GeV by using a next-to-leading order (NLO) pQCD inspired parton model, which has been very successful in describing the high p_T region physics in $p+p$ collisions [36]. Later by including the nuclear effects it is extended to consider the single hadron and di-hadron productions in $Au+Au$ collisions and has given a very good description on the high p_T pion and charged hadron productions at RHIC [37]. An interesting observation in the model shows that the ratio of gluon/quark jets in NLO is larger than in LO calculations [37]. In the same framework, we will investigate the high p_T pion and proton (anit-proton) spectra, especially the p/π ratio at $\sqrt{s} = 200$GeV. We find that with gluon energy loss larger than quark energy loss in QGP, the NLO pQCD parton model shows the ratios p/π in $Au+Au$ will be smaller than those in $p+p$ collisions, which agrees with the previous pioneer study in leading-order parton model [31]. To explain the observed p/π ratios at STAR Collaboration phenomenologically, two different scenarios in jet quenching theory are considered: one is the case that gluon energy loss is equal to quark energy loss in nuclear medium; another with a strong jet conversion mechanism where a appreciable quark jets are converted into gluon jets. Both scenarios will effectively increase the total number of final gluon jets passing through the hot QGP medium, and thus give a higher p/π ratios, which are found to reproduce the experimental data fairly well. However, $\bar{p}/p$ in the latter scenario is found to fit data better than that in the former scenario. In addition, $R^p_{AA} = R^\pi_{AA}$ is found in the former scenario while $R^p_{AA} < R^\pi_{AA}$ in the latter scenario.

The paper is organized as follows. In Sec. 2, we describe explicitly the NLO pQCD parton model in $p+p$ and $Au+Au$ collisions. The effect due to equal energy losses of the quark and gluon is taken into account in Sec. 3. In Sec . 4, the mechanism of flavor conversion between quark and gluon jet is considered. A reasonable conversion rate with which the results are in good agreement with experimental data is fixed on. Finally, we conclude in Sec. 5 with a summary of present work.

2. High p_T hadron production given by a NLO pQCD parton model

PQCD parton model has been shown to work well for large p_T particle production in high energy nucleon-nucleon collisions[38]. The factorization theorem demonstrates that the inclusive particle production cross section in $p+p$ collisions can be expressed as a convolution of parton distribution functions inside the hadron, elementary parton-parton scattering cross sections and parton fragmentation functions,

$$\frac{d\sigma^h_{pp}}{d\Gamma} = \sum_{abcd(e)} \int dx_a dx_b dz_{c(d,e)} f_{a/p}(x_a,\mu^2) f_{b/p}(x_b,\mu^2) \times \frac{1}{2x_a x_b s} \Psi(ab \to cd(e)) D_{h/c(d,e)}(z_{c(d,e)},\mu^2), \quad (1)$$

where $\Psi(ab \to cd(e))$ is related to the squared matrix elements for the various $2 \to 2$ or $2 \to 3$ subprocesses in parton-parton hard scattering. $d\Gamma$ is the differential two-body or three-body phase space element. The detailed expressions and introductions

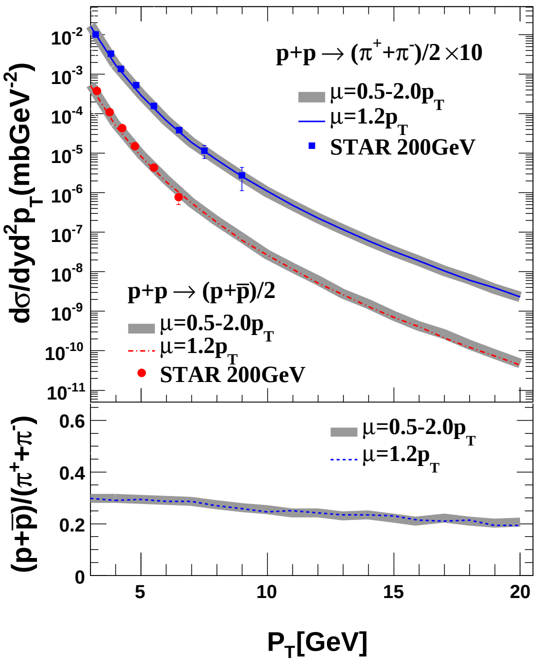

Figure 1. (Color online) The hadron spectra for $(\pi^+ + \pi^-)/2$ and $(p + \bar{p})/2$ and the ratios of $(p + \bar{p})/(\pi^+ + \pi^-)$ in $p + p$ collisions at $\sqrt{s} = 200$ GeV. Different values of the scales for factorization, renormalization and fragmentation are used in numerical calculations. The data are from Ref[32].

for $\Psi(ab \to cd(e))$ and $d\Gamma$ can be found in references [36, 39]. $f_{a/p}(x_a, \mu^2)$ is the normal parton distribution function (PDF) for which we will use the CTEQ6M parametrization [40], and x_a is the fraction of the hadron's momentum carried by the parton. $D^0_{h/c}(z_c, \mu^2)$ is the fragmentation function (FF) of parton c into hadron h, and z_c is the momentum fraction of a parton jet carried by a produced hadron. We will use mainly the updated AKK parametrization [41] for jet fragmentation, which has recently been improved from both new theoretical input and RHIC data, especially for $\pi^{\pm}$, $K^{\pm}$, $p/\bar{p}$, K^0_S and $\Lambda/\bar{\Lambda}$ particles.

The calculations discussed in this paper are carried out within a NLO Monte Carlo based program which uses a variant of the phase space slicing technique [36, 42]. This allow the same kinematic cuts in the extraction of the data to be imposed on the theoretical predictions. For the lowest-order contributions of $2 \to 2$ tree level (α_s^2 order), the NLO correction contributions (α_s^3 order) include 1-loop correction contributions to $2 \to 2$ tree level and $2 \to 3$ tree level contributions, which utilize two-cutoff parameters [36], δ_s and δ_c, to isolate the soft and collinear divergences in the squared matrix elements. The results in a set of two-body and three-body weights depend on the cut-offs, but this dependence cancels when the weights are combined in the calculation of physical observations.

For the calculations of the cross section at fixed values of the transverse momentum

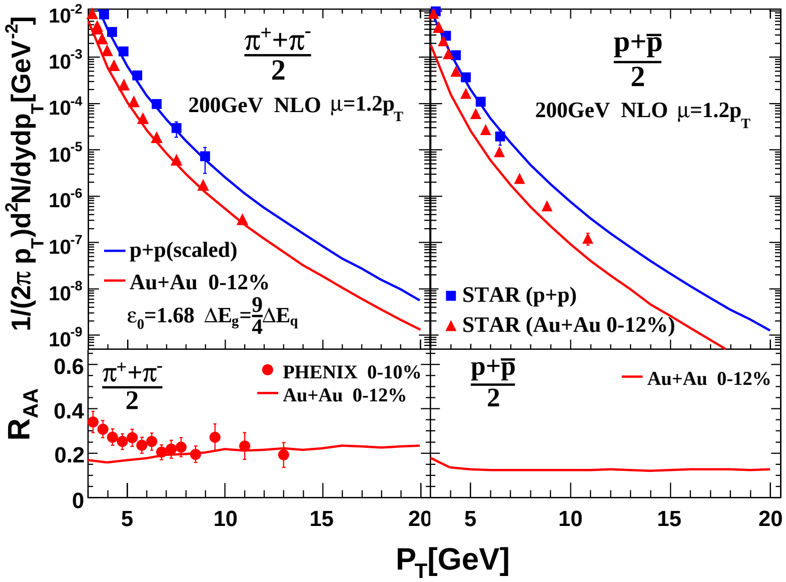

Figure 2. (Color online) The spectra of $(\pi^+ + \pi^-)/2$ and $(p + \bar{p})/2$ in $p + p$ and $Au + Au$ collisions, and the suppression factors in central $Au + Au$ collisions at $\sqrt{s} = 200GeV$. The data are from Ref.[32].

p_T of the produced hadron, we will choose the factorization scale, the renormalization scale and the fragmentation scale μ to be all proportional to p_T. As pointed out in Ref.[37], the calculated single inclusive π^0 spectra in the NLO pQCD parton model in $p+p$ collisions agree well with the experimental data at the RHIC energy with the scale in the range $\mu = 0.9 \sim 1.5p_T$. Shown in Fig. (1) we give the spectra for charged pion and (anti-)proton in $p + p$ collisions and their ratios $(p + \bar{p})/(\pi^+ + \pi^-)$ as functions of p_T. The grey bands are with scales $\mu = 0.5 - 2.0p_T$. Not only the NLO spectra but also the ratios in $p + p$ collisions are not very sensitive to the scale. So we will choose the same scale $\mu = 1.2p_T$ in the following calculations for both $p + p$ and $Au + Au$ collisions.

Assuming the $N + N$ cross section can be extrapolated to $A + A$ collisions, the inclusive invariant differential cross section for producing a hadron h in a collision of nucleuses of types A and B can be written as,

$$\begin{aligned}\frac{d\sigma^h_{AA}}{d\Gamma} = &\sum_{abcd(e)} \frac{1}{2\pi} \int d\phi db^2 dr^2 dx_a dx_b dz_{c(d,e)} \\ &\times t_A(\mathbf{r}) t_A(|\mathbf{r} - \mathbf{b}|) \\ &\times f_{a/A}(x_a, \mu^2, \mathbf{r}) f_{b/A}(x_b, \mu^2, |\mathbf{r} - \mathbf{b}|) \\ &\times \frac{1}{2x_a x_b s} \Psi(ab \to cd(e)) \\ &\times D_{h/c(d,e)}(z_{c(d,e)}, \mu^2, \Delta E_{c(d,e)}) \, , \end{aligned} \tag{2}$$

where ϕ is the azimuthal angle with respect to the reaction plane and describes the direction a final parton jet is emitted in the overlap region between two colliding nuclei.

The function $t_A(r) = \frac{3A}{2\pi R^2}\sqrt{1-r^2/R^2}$ is the nuclear thickness function in a hard-sphere geometry model, normalized to $\int d^2r t_A(r) = A$ which is the nucleon number or mass number in a nuclei with radius $R = 1.12A^{1/3}$ fm. $f_{a/A}(x_a, \mu^2, r)$ is assumed to be factorizable into the parton distribution in a free nucleon $f_{b/N}(x, \mu^2)$ and the nuclear shadowing factor $S_{a/A}(x, \mathbf{r})$ given by HIJING parameterization[43],

$$f_{a/A}(x,\mu^2,\mathbf{r}) = S_{a/A}(x,\mathbf{r})[\frac{Z}{A}f_{a/p}(x,\mu^2) + (1-\frac{Z}{A})f_{a/n}(x,\mu^2)]\,, \tag{3}$$

where we have explicitly taken into account the isospin of the nucleus by considering the parton distributions of a neutron which are obtained from that of a proton by isospin symmetry.

As assumed in Ref. [28, 37], the effect of final-state interaction between produced parton and the bulk medium can be described by the effective medium-modified FF's,

$$D_{h/c}(z_c,\Delta E_c,\mu^2) = (1-e^{-\langle\frac{L}{\lambda}\rangle})\left[\frac{z'_c}{z_c}D^0_{h/c}(z'_c,\mu^2) + \langle\frac{L}{\lambda}\rangle\frac{z'_g}{z_c}D^0_{h/g}(z'_g,\mu^2)\right] + e^{-\langle\frac{L}{\lambda}\rangle}D^0_{h/c}(z_c,\mu^2), \tag{4}$$

where $z'_c = p_T/(p_{Tc} - \Delta E_c)$, $z'_g = \langle L/\lambda\rangle p_T/\Delta E_c$ are the rescaled momentum fractions, ΔE_c is the average radiative parton energy loss and $\langle L/\lambda\rangle$ is the number of scatterings along the parton propagating path,

$$\langle L/\lambda\rangle = \int_{\tau_0}^{\infty}\frac{d\tau}{\rho_0\lambda_0}\rho_g(\tau,\mathbf{b},\mathbf{r}+\mathbf{n}\tau). \tag{5}$$

Neglecting transverse expansion, the gluon density distribution in a 1-d expanding medium in $A+A$ collisions at impact-parameter $\mathbf{b}$ is assumed to be proportional to the transverse profile of participant nucleons,

$$\rho_g(\tau,\mathbf{b},\mathbf{r}) = \frac{\tau_0\rho_0}{\tau}\frac{\pi R_A^2}{2A}[t_A(\mathbf{r}) + t_A(|\mathbf{b}-\mathbf{r}|)]. \tag{6}$$

According to recent theoretical studies [11, 18, 44] the total parton energy loss in a finite and expanding medium can be approximated as a path integral,

$$\Delta E \approx \langle\frac{dE}{dL}\rangle_{1d}\int_{\tau_0}^{\infty}d\tau\frac{\tau-\tau_0}{\tau_0\rho_0}\rho_g(\tau,\mathbf{b},\mathbf{r}+\mathbf{n}\tau), \tag{7}$$

for a parton produced at a transverse position $\mathbf{r}$ and traveling along the direction $\mathbf{n}$. $\langle dE/dL\rangle_{1d}$ is the average parton energy loss per unit length in a 1-d expanding medium with an initial uniform gluon density ρ_0 at a formation time τ_0 for the medium gluons. The energy dependence of the energy loss is parameterized as

$$\langle\frac{dE}{dL}\rangle_{1d} = \epsilon_0(E/\mu_0 - 1.6)^{1.2}/(7.5 + E/\mu_0), \tag{8}$$

from the numerical results in Ref. [44] in which thermal gluon absorption is also taken into account. The parameter ϵ_0 should be proportional to the initial gluon density ρ_0.

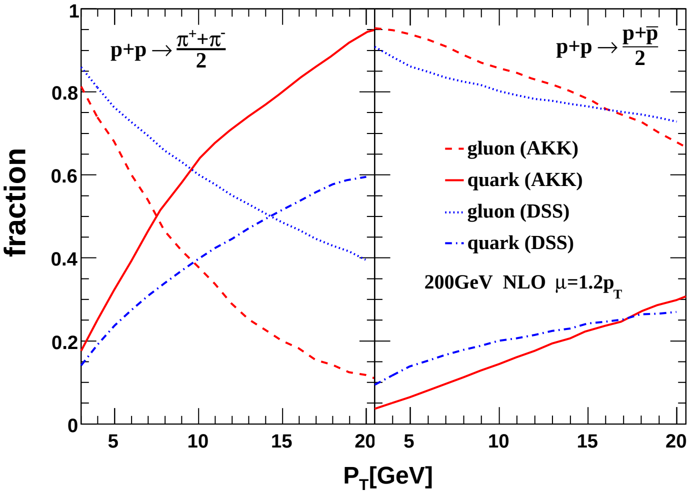

Figure 3. (Color online) The fractions of contributions to the charged π and (anti-)proton from quark and gluon jets with AKK fragmentation functions and DSS fragmentation functions in $p + p$ collisions at $\sqrt{s} = 200$ GeV, respectively.

A simultaneous fit to the single and dihadron data constrains the energy loss parameter within a narrow range: $\epsilon_0 = 1.6 - 2.1$ GeV/fm in Ref.[37]. For the following calculations we will choose the same parameters as in the reference, $\mu_0 = 1.5$ GeV, $\epsilon_0\lambda_0 = 0.5$ GeV and $\tau_0 = 0.2$ fm in $Au + Au$ collisions at $\sqrt{s} = 200$ GeV.

Shown in Fig. (2) are the charged π and (anti-)proton spectra and the suppression factors in central $Au + Au$ collisions at $\sqrt{s} = 200$ GeV. The suppression factor (or nuclear modification factor) which mainly manifests jet quenching effect in our current studies is defined as [45],

$$R_{AA} = \frac{d\sigma^h_{AA}/dyd^2p_T}{\langle N_{binary}\rangle d\sigma^h_{pp}/dyd^2p_T}, \tag{9}$$

where N_{binary} is the average number of geometrical binary collisions at a given range of impact parameters, $\langle N_{binary}\rangle = \int d^2bd^2rt_A(r)t_A(|\mathbf{b} - \mathbf{r}|)$.

Non-Abelian feature of QCD show that gluon energy loss is 9/4 times of quark energy loss in the dense matter due to the difference of color factors for gluon-gluon vertex and quark-gluon vertex [7, 29, 30]. With the parton energy loss, $\Delta E_g = 9/4\Delta E_q$, and the energy loss parameter chosen as $\epsilon_0 = 1.68$ GeV/fm, the calculated large transverse momentum $(\pi^+ + \pi^-)/2$ spectra in central $Au + Au$ collisions fit data well and the large transverse momentum $(p + \bar{p})/2$ spectra fit data bad in Fig. (2). Also shown in the figure are the suppression factors for $(\pi^+ + \pi^-)/2$ and $(p + \bar{p})/2$ spectra in central $Au + Au$ collisions, respectively. The former is found larger than the latter.

Shown in Fig.(3) are the fractions of the contributions to the charged pion and (anti-)proton from quark and gluon jets with different fragmentation functions, respectively. In the two plots the red solid curves and the red dashing curves are with AKK fragmentation functions[41] while the blue dotted curves and the blue dashed-dotted

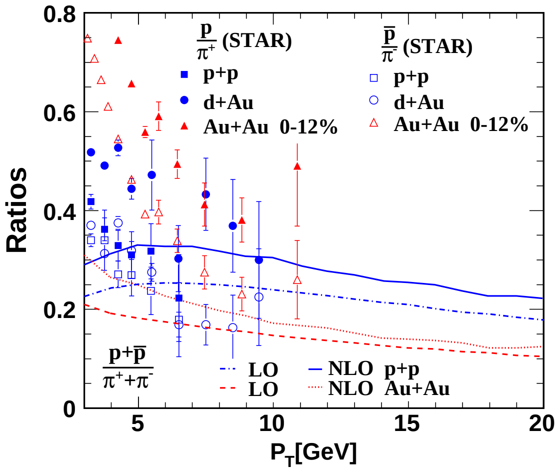

Figure 4. (Color online) The ratios of $(p+\bar{p})/(\pi^{+}+\pi^{-})$ in $p+p$ and 0-12% $Au+Au$ collisions at $\sqrt{s}=200$ GeV. The energy loss parameter is chosen as $\epsilon_0=1.68$ GeV/fm. The gluon energy loss is considered as about 2 times of the quark energy loss.

curves are with DSS fragmentation functions[46]. With the two sets of fragmentation functions, our NLO numerical results show that high p_T (anti-)proton is dominated by gluon fragmentation whereas high p_T charged pion is dominated by quark fragmentation. It is consistent with a previous study based on Monte Carlo simulations[31].

Because the gluon energy loss is considered as 9/4 times of the quark energy loss, the contribution from gluon jets is suppressed more greatly than the contribution from quark jets in central $Au+Au$ collisions. The non-Abelian feature of parton energy loss causes to a smaller suppression factor R_{AA} for large transverse momentum $(p+\bar{p})/2$ than that for $(\pi^{+}+\pi^{-})/2$, as shown in Fig. (2). So a smaller p/π ratio at high p_T in central $Au+Au$ collisions than that in $p+p$ collisions is obtained, as shown in Fig. (4). These conclusions had been previously pointed out in Ref. [31] within LO pQCD parton model.

Since the number ratio of gluon/quark jets created in hard scattering processes in NLO calculations is larger than in LO calculations [37], the contribution fraction from gluon jets will be enhanced in NLO compared with that in LO. Therefore, the NLO p/π ratio is larger than the LO ratio in both $p+p$ and central $Au+Au$ collisions. However, even in NLO calculations the p/π ratio in central $Au+Au$ collisions is still smaller than that in $p+p$ collisions, as shown in Fig.(4), while recent STAR data indicate that p/π^{+} and $\bar{p}/\pi^{-}$ ratios at high p_T in central $Au+Au$ collisions [32] approach those in $p+p$ and $d+Au$ collisions [33]. To solve this discrepancy between the theoretical calculations and experiment measurements, we will explore two scenarios: one is that gluon jets lose the same amount of energy as quark jets; another is jet conversion between gluon and quark jets. In the following we demonstrate that how p/π and $p/\bar{p}$ ratios will be modified in these two scenarios, and their comparisons with the experimental data.

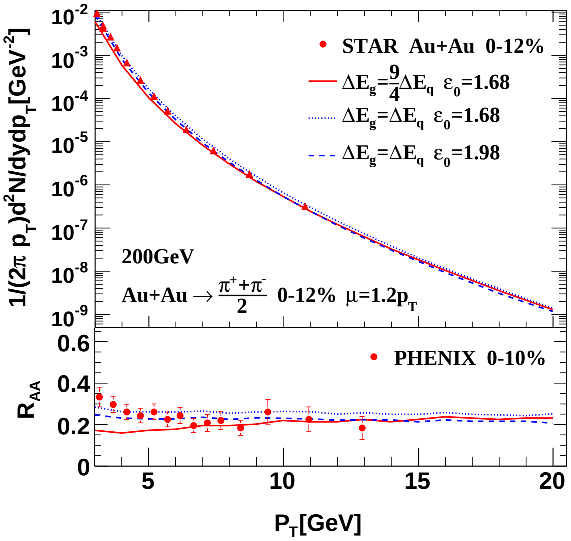

Figure 5. (Color online) The charged π meson spectra (upper) and the suppression factors (lower) with 2 sets of parton energy loss ($\Delta E_g = 9/4\Delta E_q$ and $\Delta E_g = \Delta E_q$) in central $Au + Au$ collisions at $\sqrt{s} = 200$ GeV. The data points are from [33, 47].

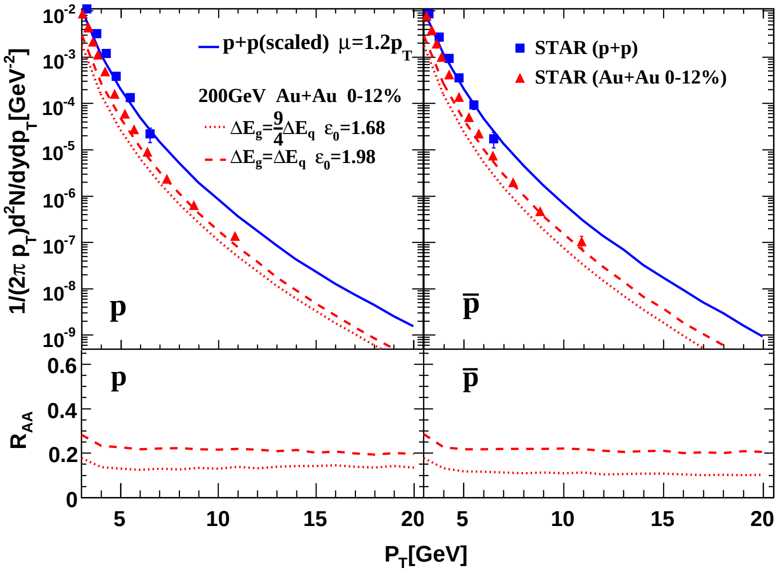

Figure 6. (Color online) The separated p and $\bar{p}$ spectra and the suppression factors in central $Au + Au$ collisions at $\sqrt{s} = 200$ GeV. The data are from [33, 47].

3. Scenario I: gluon jet energy loss is equal to quark jet energy loss

To explain phenomenologically the observed p/π ratios given by STAR Collaboration, we first consider a case in jet quenching theory: equal energy loss for both gluon and quark jets. Though currently there is no such a theory of jet quenching to justify that gluons will lose the same amount of energy as quarks, this toy model could shed light on the flavor dependence of parton energy loss in nuclear. We note such a scenario of parton energy loss had been explored in a study of the sensitivity of hadron spectra suppression to the non-Abelian parton energy loss [48].

The hadron yield will be less suppressed with parton energy loss $\Delta E_g = \Delta E_q$ than that with parton energy loss $\Delta E_g = \frac{9}{4}\Delta E_q$ in central $Au + Au$ collisions, so one should enlarge the energy loss parameter ϵ_0 to fit data. Shown in Fig. (5) are the numerical results with 2 sets of parton energy loss ($\Delta E_g = \frac{9}{4}\Delta E_q$ and $\Delta E_g = \Delta E_q$) for charged pion meson spectra and the corresponding suppression factors compared with data. From the suppression factors in Fig. (5), it is clear that $\epsilon_0 = 1.98$ GeV/fm works well for fitting data. The parameter value will be used to give (anti-)proton spectra with parton energy loss $\Delta E_g = \Delta E_q$ in central $Au + Au$ collisions.

AKK parametrization of fragmentation functions just give parton fragmentation functions to $(\pi^+ + \pi^-)/2$ or $(p + \bar{p})/2$. To get ratios p/π^+, $\bar{p}/\pi^-$ and $p/\bar{p}$ we need the parton fragmentation function to π^+, π^-, p and $\bar{p}$ respectively. Theoretical and experimental studies [32, 33, 34, 49] show that the fragmentation of quark and anti-quark jets produce mainly protons and anti-protons, respectively, and gluon jets contribute to protons and anti-protons equally. As in Ref. [33, 34], we assume that no anti-protons are produced from a quark jet and no protons are produced from an anti-quark jet. We further assume that high p_T charged π^+ and π^- mesons are equally produced from hard parton jet fragmentations, consistent with experiment findings [32, 33].

Based on the NLO pQCD parton model, we calculate the separated proton and anti-proton spectra with the energy loss parameter $\epsilon_0 = 1.98$ GeV/fm and the equal energy loss for both gluon and quark jets in central $Au + Au$ collisions at $\sqrt{s} = 200$ GeV. The numerical results are shown in Fig. (6) where the suppression factors are also included. The equal energy loss for both gluon and quark jets for (anti-)proton production in central $Au + Au$ collisions results in the suppression factor $R^p_{AA} \approx 0.2$, equal to $R^\pi_{AA} \approx 0.2$ shown in Fig. (5). As shown in Fig. (3), high p_T (anti-)proton production is dominated by gluon fragmentation. Compared with the case of parton energy loss $\Delta E_g = \frac{9}{4}\Delta E_q$, gluon jets with less energy loss $\Delta E_g = \Delta E_q$ may have larger probability to pass through the hot medium and this gives a larger percentage of contribution for (anti-)proton production, so one can see in Fig. (6) that (anti-)proton spectra with parton ernergy loss $\Delta E_g = \Delta E_q$ are enhanced although the energy loss parameter ϵ_0 is adjusted large to 1.98 GeV/fm instead of 1.68 GeV/fm.

Shown in Fig. (7) are $\bar{p}/p$ ratios in $p + p$ and central $Au + Au$ collisions at $\sqrt{s} = 200$ GeV. According to our NLO calculations on the fractions of contributions to (anti-)proton from the fragmentaions of quark and gluon jets shown in Fig. (3), one know that the ratio of gluon to quark jet contributing to (anti-)proton production decreases with the (anti-)proton transverse momentum. Because most of antiprotons come from gluons while protons come from both valence quark and gluon fragmentation [31], the ratio of antiproton to proton production cross section should also decrease with their p_T , as our NLO calculations show in Fig. (7). Similar to the LO calculations in Ref. [31],

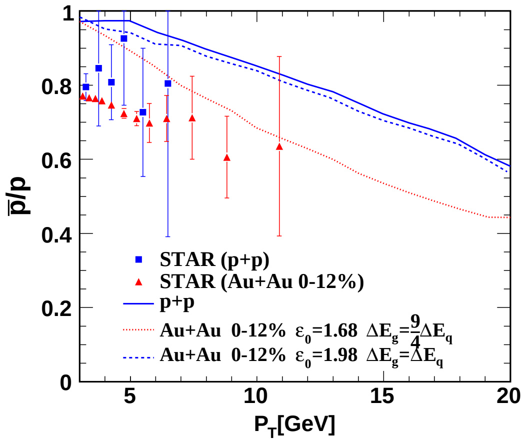

Figure 7. (Color online) The $\bar{p}/p$ ratios at mid-rapidity ($|y| < 0.5$) as functions of p_T in $p + p$ (solid curve) and $0 - 12\%$ $Au + Au$ collisions at $\sqrt{s} = 200$ GeV. The data are from [32, 33].

the ratio will always be smaller than 1 because there are much more quark jets than anti-quark jets produced in hard scattering in $p + p$ collisions due to baryon number conservation. In central $Au + Au$ collisions the non-Abelian feature of parton energy loss ($\Delta E_g = 9/4\Delta E_q$) reduces the contribution proportion from gluon jet fragmentations compared with that in $p + p$ collisions, so the large transverse momentum $\bar{p}/p$ ratio in central $Au+Au$ collisions is found to be smaller than that in $p+p$ collisions. If gluon jets lose less energy ($\Delta E_g = \Delta E_q$ instead of $\Delta E_g = 9/4\Delta E_q$), the contribution from gluon jet fragmentations is enhanced, therefore there is a larger $\bar{p}/p$ ratio with $\Delta E_g = \Delta E_q$ than that with $\Delta E_g = 9/4\Delta E_q$ in central $Au + Au$ collisions. In another point of view, equal energy loss for both quark and gluon jets causes to equal suppression for both p and $\bar{p}$ spectra (shown in Fig. (6)), so the large transverse momentum $\bar{p}/p$ ratio with $\Delta E_g = \Delta E_q$ in central $Au + Au$ collisions is equal to that in $p + p$ collisions.

In Fig. (8) we make a comparison of $p(\bar{p})/\pi^+(\pi^-)$ ratios with 2 sets of parton energy loss ($\Delta E_g = 9/4\Delta E_q$ and $\Delta E_g = \Delta E_q$) in central $Au + Au$ collsions at $\sqrt{s} = 200$ GeV. On one hand, if gluon jets lose less energy ($\Delta E_g = \Delta E_q$ instead of $\Delta E_g = 9/4\Delta E_q$), more gluon jets are survived to contribute to hadron production when they encounter multiple scattering in the hot and dense matter created in central $Au + Au$ collisions. The gluon contribution has an enhanced fraction while the quark contribution has a reduced fraction, and because high p_T proton (anti-proton) production is dominated by gluon fragmentation whereas high p_T pion is dominated by quark fragmentation, the $p(\bar{p})/\pi^+(\pi^-)$ ratios with $\Delta E_g = \Delta E_q$ are larger than those with $\Delta E_g = 9/4\Delta E_q$ shown in Fig. (8). On the other hand, equal energy loss for both quark and gluon jets washes out the suppression difference between (anti-)proton and pion spectra, $R^p_{AA}(p_T) \approx R^\pi_{AA}(p_T)$, shown in Fig. (5) and (6). In fact, the p/π ratio with parton energy loss $\Delta E_g = \Delta E_q$ in

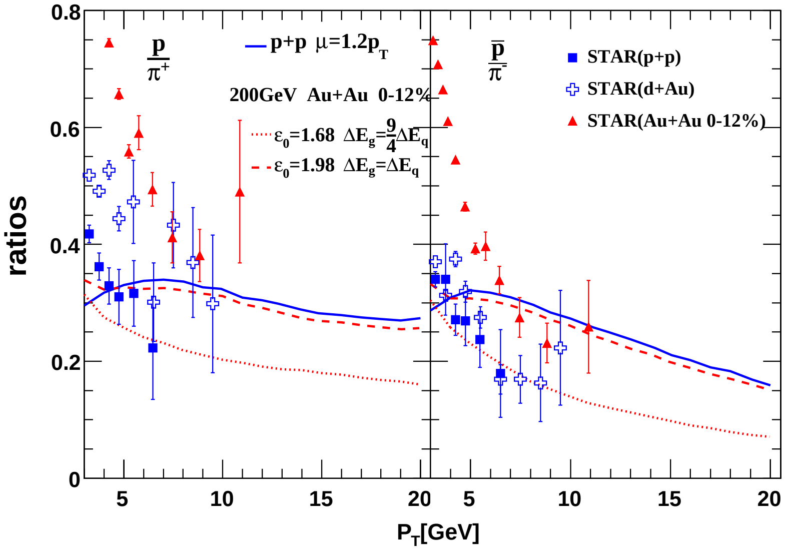

Figure 8. (Color online) The p/π^+ and $\bar{p}/\pi^-$ ratios at mid-rapidity($|y| < 0.5$) as functions of p_T in $p+p$ collisions (solid line) and $0-12\%$ $Au+Au$ collisions at $\sqrt{s} = 200$ GeV. The data are from [32, 33].

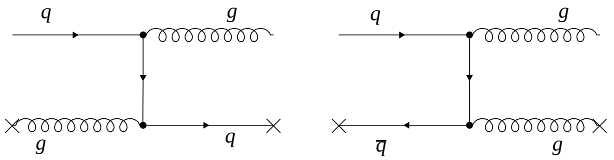

(a.) (b.)

Figure 9. Conversions between quark and gluon jets via both elastic $gq(\bar{q}) \to q(\bar{q})g$ and inelastic $q\bar{q} \leftrightarrow gg$ scatterings with thermal quarks and gluons in the hot and dense matter.

central $Au + Au$ collisions can be written as

$$(\frac{p}{\pi})^{AuAu} = (\frac{R_{AA}^{p}}{R_{AA}^{\pi}})(\frac{p}{\pi})^{pp} \approx (\frac{p}{\pi})^{pp}. \tag{10}$$

That's why our numerical results for large transverse momentum p/π ratios with $\Delta E_g = \Delta E_q$ in central $Au+Au$ collisions approach to those in $p+p$ collisions, consistent with experiment findings[32, 33] shown in Fig. (8).

4. Scenario II: Strong Conversion between hard quark and gluon jets

The conversion between quark and gluon jets is a mechanism introduced in Ref.[34, 35] to explain the discrepancy for p/π ratios between the experimental data and the theoretical calculations. Although a conversion enhancement factor $K = 4 \sim 6$ would be needed to explain experimental data observed by STAR and further theoretical studies will be needed to understand how we can get such a large conversion enhancement factor,

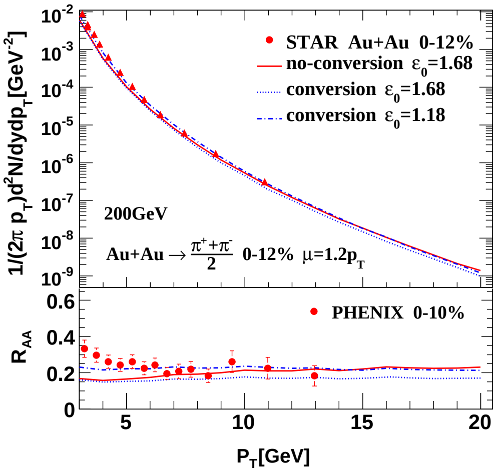

Figure 10. (Color Online) The charged pion spectra and nuclear modification factors with and without conversion in central $Au + Au$ collisions at $\sqrt{s} = 200$ GeV. The data are from [33, 47].

this mechanism indeed leads to an increase in the final number of gluon jets in central $Au + Au$ collisions than the case without conversions [34], and thus provide a promising way to explain the striking experimental data on proton over pion ratio observed at STAR collaboration [32]. In this section we will apply the jet conversion mechanism into the NLO pQCD parton model to study (anti-)proton and charged pion spectra and their ratios in heavy ion collisions.

Conversions between quark and gluon jets could happen via both elastic $gq(\bar{q}) \rightarrow q(\bar{q})g$ and inelastic $q\bar{q} \leftrightarrow gg$ scatterings with thermal quarks and gluons in the hot and dense matter as illustrated in Fig. (9). For a parton jet created at a spatial point in $Au + Au$ collisions region and escaping out off the dense matter in the transverse plane, multiple scattering with the medium particles wears off the jet energy and also stimulates the jet to convert to its partner. The conversion possibility for the jet passing through the matter is in turn connected with its energy and the medium particle density distributed along its passing path.

As studied in Ref. [34, 50], the quark-to-gluon conversion possibility is found to be larger than the gluon-to-quark possibility at the same jet energy, and about 30% quarks for net quark-to-gluon jet conversions are needed to account for the observed ratios in the experiment in central $Au + Au$ collisions. For simple evaluation for net quark-to-gluon conversions, we neglect gluon-to-quark jet conversions, and assume the quark-to-gluon jet conversion has an averaged possibility 45% all over its path. In our actual calculation, the quark and gluon jet contributions to the observed hadrons can be separated within a NLO pQCD parton model in A+A collisions. Once quark jets are created anywhere inside the medium, 45% quark jets are marked as gluon jets who will encounter multiple scattering and then fragment into hadrons. After a quark-to-gluon jet conversion happens at some point on the path in the medium, the newcomer (gluon)

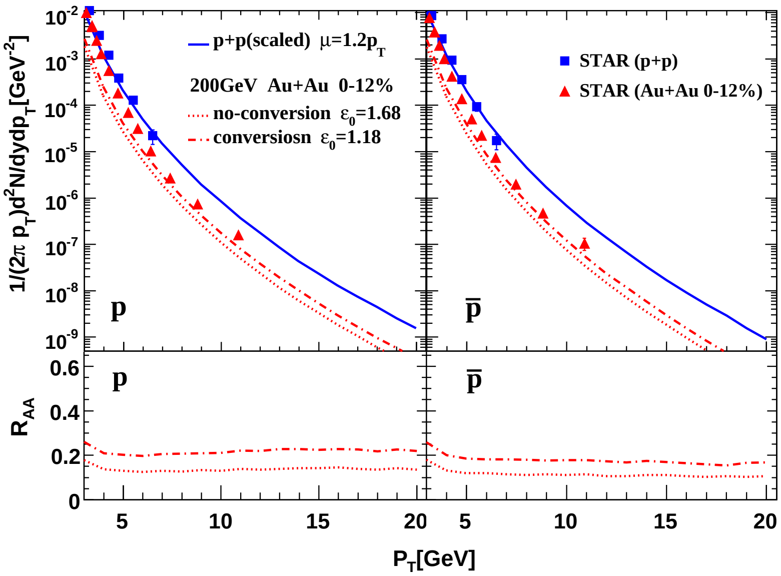

Figure 11. (Color online) The separated p and $\bar{p}$ spectra and the suppression factors with and without conversion in central $Au + Au$ collisions at $\sqrt{s} = 200$ GeV. The data are from [33, 47].

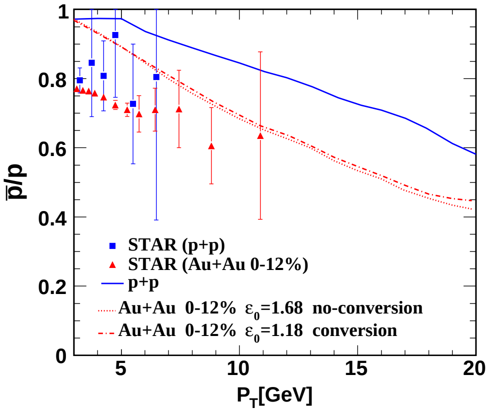

Figure 12. (Color online) The $\bar{p}/p$ ratio at mid-rapidity($|y| < 0.5$) as functions of p_T in $p + p$ (solid curve)and $0 - 12\%$ $Au + Au$ (with and without conversion) collisions at $\sqrt{s} = 200$ GeV. The data are from [32, 33].

will have energy loss $\Delta E_g = 9/4 \Delta E_q$ different from the energy loss ΔE_q for its parent jet (quark). Because the "new" gluon is easier absorbed by the hot and dense matter than the parent quark, the total jet number will be reduced by net quark-to-gluon conversions, and there are actually about 30% of final surviving conversion jets. The ratio 30% is consistent to the studies in Ref. [34, 50]. In our calculations jet energy loss depends on the local parton density and total propagation length. A more sophisticated consideration will be needed in the further studies for the net quark-to-gluon conversion

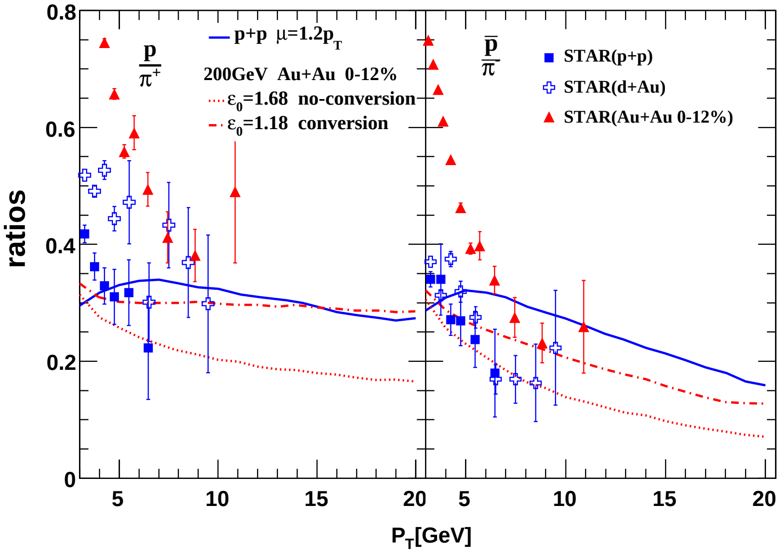

Figure 13. (Color online) The p/π^+ and $\bar{p}/\pi^-$ ratios at mid-rapidity($|y| < 0.5$) as functions of p_T in $p+p$ and central $Au+Au$ collisions with conversion (dotted-dashed line) and without conversion (dotted line) between quarks and gluons. Data points are taken from [32, 33].

dependent on the local parton density and total propagation length.

The appearance of net quark-to-gluon jet conversions will increase the total number of final gluon jets passing through the hot QGP medium. In such a conversion framework with gluon energy loss larger than quark energy loss, $\Delta E_g = 9/4 \Delta E_q$, the high p_T hadron yield should be smaller than that without conversion. To fit data for hadron spectra, the energy loss parameter ϵ_0 should be adjusted to be smaller than 1.68 GeV/fm.

Shown in Fig. (10) are the charged pion spectra and nuclear modification factors with and without conversion in central $Au + Au$ collisions at $\sqrt{s} = 200$ GeV. Our numerical results with conversion mechanism and $\epsilon_0 = 1.18$ GeV/fm are found to fit data well. With this energy loss parameter we then show in Fig. (11) separately p and $\bar{p}$ spectra and the suppression factors with and without conversion in central $Au + Au$ collisions. The spectra with conversion are found to fit data better than without conversion, and the nuclear modification factor for proton production with conversion in Fig. (11) is similar to that with conversion for pion production in Fig. (10), $R^p_{AA} \approx R^\pi_{AA}$ due to the increasing number of converted gluon jets which dominate proton productions. However, R_{AA} for anti-proton with conversion is slightly smaller than that for proton with conversion, $R^{\bar{p}}_{AA}/R^p_{AA} \approx 0.75$, because most of antiprotons come from gluons with energy loss larger than quark while protons come from both valence quark and gluon fragmentation.

In Fig. (12) we plot the $\bar{p}/p$ ratio as a function of p_T in $p + p$ (solid curve) and central $Au + Au$ (with and without conversion) collisions. Of interest is that the ratio $\bar{p}/p$ with conversion is found to be approximately equal to that without conversion, and fit data better than $\bar{p}/p$ in the scenario of equal energy loss for both quark and gluon jets in central $Au + Au$ collisions. In fact, according to the result in Fig. (11), $R^{\bar{p}}_{AA}/R^{p}_{AA} \approx 0.75$, one can obtain $(\bar{p}/p)_{AuAu} \approx 0.75(\bar{p}/p)_{pp}$, consistent with the numerical results in Fig. (12). The net quark-to-gluon jet conversions enhance the total number of the final gluon jets as compared with no conversion, and most of antiprotons come from gluons while protons come from both valence quark and gluon fragmentation, so the ratio $\bar{p}/p$ with conversion should be smaller than that with no conversion. But compared with the no conversion case with $\epsilon_0 = 1.68$ GeV/fm, the smaller energy loss parameter $\epsilon_0 = 1.18$ GeV/fm for the conversion case should give rise to the $\bar{p}/p$ curve for the conversion case a bit closer to the curve for the $p + p$ case. Therefore, the ratio $\bar{p}/p$ with conversion is found to be approximately equal to that with no conversion in central $Au + Au$ collisions.

Shown in Fig. (13) are the p/π^+ and $\bar{p}/\pi^-$ ratios in $p + p$ and central $Au + Au$ collisions with conversion (dotted-dashed line) and without conversion (dotted line) between quarks and gluons. The ratios of (anti)-proton over pion with conversion are found to fit data not bad. Net quark-to-gluon jet conversions effectively increase the total number of final gluon jets surviving in the fire ball. Therefore the final fractions of gluon and quark jets contributing to the hadron spectra will be modified by the net quark-to-gluon conversion. Furthermore, our numerical results in Fig. (3) show that even if without net quark-to-gluon conversions high p_T proton (anti-proton) production is dominated by gluon fragmentations whereas high p_T pion is dominated by quark fragmentations in central $Au + Au$ collisions. Consequently, larger p/π ratios are found in central $Au + Au$ collisions with conversion than without conversion, $(\frac{\bar{p}}{\pi^-})^{conv.}_{AuAu} > (\frac{\bar{p}}{\pi^-})^{no\ conv.}_{AuAu}$ and $(\frac{p}{\pi^+})^{conv.}_{AuAu} > (\frac{p}{\pi^+})^{no\ conv.}_{AuAu}$ shown in Fig. (13). Similar to the case in Fig.(4), the ratios of (anti)-proton over pion in central $Au + Au$ collisions with conversion are smaller than those in $p + p$ collisions. According to $R^{\bar{p}}_{AA} < R^{p}_{AA} \approx R^{\pi^+}_{AA} (= R^{\pi^-}_{AA})$ from Fig. (10)(11), one can get

$$(\frac{p}{\pi^+})^{AuAu} = (\frac{R^{p}_{AA}}{R^{\pi^+}_{AA}})(\frac{p}{\pi^+})^{pp} \approx (\frac{p}{\pi^+})^{pp}; \tag{11}$$

$$(\frac{\bar{p}}{\pi^-})^{AuAu} = (\frac{R^{\bar{p}}_{AA}}{R^{\pi^-}_{AA}})(\frac{\bar{p}}{\pi^-})^{pp} < (\frac{\bar{p}}{\pi^-})^{pp}, \tag{12}$$

as one can see in Fig. (13). p/π^+ ratios in central $Au + Au$ collisions with conversion are similar to those in $p + p$ collisions. However $\bar{p}/\pi^-$ ratios in central $Au + Au$ collisions with conversion are smaller than those in $p + p$ collisions because the number of anti-quark jets is smaller than that of quark jets and the effect of conversion mechanism is not obvious for anti-quark jets.

We note that in the conventional jet quenching theory, because a gluon jet always lose more energy than a quark jet with the same initial energy in a hot QCD medium (except in the case when both quark jet and gluon jet lose all of their energies), and at high p_T π meson is dominated by valence quark fragmentation whereas proton is dominated by gluon fragmentation, the p/π ratio at large transverse momentum in $p + p$ collision should be no less than those in $A + A$ collisions. The two scenarios considered in this paper will raise the p/π ratios in $A + A$ collisions therefore becoming closer to those in $p + p$, but will never go beyond. Only in the extreme case in $A + A$ collisions at large p_T, all quark jets are converted into gluon jets, or equivalently there are only gluon jets, we can get higher p/π ratio in $A + A$ collisions at large p_T. Though current data at STAR seems to imply that proton over pion ratio in $Au + Au$ reactions is enhanced relative to that in $p + p$ collisions, with large error bars at high p_T, we still can not reach a unambiguous conclusion. If in the future more accurate experimental measurements confirm that at high p_T region, p/π ration in $A + A$ collision is enhanced significant compared with that in $p+p$ collision, a dramatic change of our understanding of parton energy loss mechanism will be needed. Because we focus on p/π ratios at the high p_T region, in our calculations we have ignored the contribution of parton recombination/coalescence mechanism in the QGP. We expect this negligence underlines the rather large discrepancy between our numerical simulations and experimental data in the intermediate p_T region, where the recombination/coalescence mechanism in the hot QGP should play a very important role [51, 52, 53, 54, 55].

5. Summary and discussions

In this paper, we investigate p/π^+ and $\bar{p}/\pi^-$ ratios at large transverse momentum in $Au + Au$ collisions with jet quenching based on an next-to-leading order pQCD parton model. Two scenarios are considered to explain the anomaly of p/π ratios observed by STAR Collaboration that p/π ratios at high p_T in central $Au + Au$ collisions [32] approach those in $p+p$ and $d+Au$ collisions [33]. Firstly, we investigate the consequence in Scenario I where gluons lose the same amount of energy in QGP as quarks and demonstrate that it will enhance the p/π^+ and $\bar{p}/\pi^-$ ratios for central $Au+Au$ collisions. Secondly, we explore the effect of strong jet conversion in Scenario II where a net of quark-to-gluon conversion also result in similar p/π^+ and $\bar{p}/\pi^-$ ratios in central $Au+Au$ and $p+p$ collisions. In both scenarios, the final number of gluon jets passing through the hot and dense medium is increased as compared to the original jet quenching picture, and jet conversion scenario is favorable when $p/\bar{p}$ ratio is considered because $\bar{p}/p$ in the latter scenario is found to fit data better than that in the former scenario. This kind of studies should improve our understanding on the flavor dependence of energy loss and lead us to a unified picture of jet quenching.

We note that in our approach the effect of energy loss is taken into account through the medium-modified effective fragmentation functions and the evolution of the hot nuclear medium is described by a simple 1+1D Bjorken evolution based on Hard-Sphere geometry. This approach has given very well descriptions on inclusive pion suppression [44], di-hadron production [37] and photon-tagged hadron production [56], but several improvements will be needed to make a more realistic consideration of parton energy loss in the hot medium created at RHIC. One direction is to simulate the medium evolution with the 3+1D hydrodynamics model as in Ref. [57, 58], which may give corrections to the total parton energy loss though the effect of local density dropping due to the transverse expansion of the medium will be offset by the longer path length in the transverse direction [59] in the QGP phase‡. Also one could study the in-medium parton shower [57, 61, 62] to make a more differential study of jet quenching than the adoption of the effectively modified parton fragmentation function. Furthermore a more detailed medium dependence of jet energy loss can be obtained by introducing the energy loss probability distributions [57, 58, 63, 64, 65], which will reduce the difference of energy losses of quark and gluon jets by properly incorporating kinematical constraints, and thus raise the p/π ratios. Last but not the least, in our calculation we have assumed that the pions and protons are formed outside of the medium, and the hadronization of pions and protons in A+A collisions are the same as that in p+p collisions. Larger p/π ratios may be obtained and help to resolve the p/π puzzles observed in A+A collisions at STAR if one assumes that protons in A+A collisions can be formed inside the medium due to its larger mass relative to pion , though so far how to model hadronizations of partons with large p_T in medium and whether it is distinct from that in vacuum is still an open question and under hot debate. Nevertheless, intensive theoretical studies will be needed to see whether we can resolve the puzzle of p/π ratios in a more beautiful and natural way by improving our model and including all the relevant effects discussed above.

This work was supported by NSFC of China under Projects No. 10825523 and No. 10875052 and No. 10635020, by MOE of China under Projects No. IRT0624; by MOST of China under Project No. 2008CB317106; and by MOE and SAFEA of China under Project No. PITDU-B08033.

References

[1] Arsene I *et al.* (BRAHMS Collaboration) 2005 Nucl. Phys. A **757** 1
[2] Back B-B *et al.* (PHOBOS Collaboration) 2005 Nucl. Phys. A **757** 28
[3] Adams J *et al.* (STAR Collaboration) 2005 Nucl. Phys. A **757** 102
[4] Adcox K *et al.* (PHENIX Collaboration) 2005 Nucl. Phys. A **757** 184
[5] Adams J *et al.* (STAR Collaboration) 2003 Phys. Rev. Lett. **91** 072304; 2003 **91** 172302
[6] Adler S-S *et al.* (PHENIX Collaboration) 2003 Phys. Rev. Lett. **91** 072301
[7] Wang X-N and Gyulassy M 1992 Phys. Rev. Lett. **68** 1480; 1994 Nucl. Phys. **B420** 583
[8] Wang X-N 2004 Phys. Lett. **B579** 299
[9] Plüemer M, Gyulassy M and Wang X-N 1995 Nucl. Phys. **A590** 511C
[10] Wang X-N 2001 Phys. Rev. C **63** 054902
[11] Gyulassy M, Vitev I and Wang X-N 2001 Phys. Rev. Lett. **86** 2537
[12] Adler C *et al.* 2003 Phys. Rev. Lett. **90** 082302
[13] Guo X-F and Wang X-N 2000 Phys. Rev. Lett. **85** 3591
[14] Zhang B-W and Wang X-N 2003 Nucl. Phys. A **720** 429
[15] Majumder A, Wang E and Wang X-N 2007 Phys. Rev. Lett. **99** 152301

---

‡ In other phases of 3+1D hydrodynamical evolution, for instance in the mixed phase (MP), the path length may shorten with the transverse expansion of the system[60], and we thank the referee for pointing out this anomaly of path length variation with the transverse expansion at the full 3+1D hydrodynamics simulation.

[16] Majumder A, Fries R-J and Muller B 2008 Phys. Rev. C **77** 065209
[17] Wiedemann U-A 2000 Nucl. Phys. **B582** 409
[18] Wiedemann U-A 2000 Nucl. Phys. **B588** 303
[19] Salgado C-A and Wiedemann U-A 2002 Phys. Rev. Lett. **89** 092303
[20] Armesto N, Salgado C-A and Wiedemann U-A 2005 Phys. Rev. Lett. **94** 022002
[21] Arnold P, Moore G-D and Yaffe L-G 2001 J. High Energy Phys.**11** 057
[22] Arnold P, Moore G-D and Yaffe L-G 2001 J. High Energy Phys.**11** 001
[23] Turbide S, Gale C, Jeon S and Moore G-D 2005 Phys. Rev. C **72** 014906
[24] Gyulassy M, Levai P and Vitev I 2000 Nucl. Phys. **B571** 197
[25] Gyulassy M, Levai P and Vitev I 2001 Nucl. Phys. **B594** 371
[26] Djordjevic M and Gyulassy M 2004 Nucl. Phys. **A733** 265
[27] Wicks S, Horowitz W, Djordjevic M and Gyulassy M 2007 Nucl. Phys. **A784**, 426
[28] Wang X-N 2004 Phys. Lett. **B595** 165
[29] Baier R, Schiff D and Zakharov B-G 2000 Ann. Rev. Nucl. Part. Sci. **50** 37
[30] Gyulassy M, Vitev I, Wang X-N and Zhang B-W arXiv:nucl-th/0302077
[31] Wang X-N 1998 Phys. Rev. C **58** 2321
[32] Adams J *et al.* (STAR Collaboration) 2006 Phys. Rev. Lett. **97** 152301; Abelev B-I *et al.* (STAR Collaboration) 2007 Phys. Lett. B **655** 104; Bedangadas Mohanty for the STAR Collaboration arXiv:nucl-ex/0705.0953
[33] Adams J *et al.* (STAR Collaboration) 2006 Phys. Lett. **B637** 161
[34] Liu W, Ko C-M and Zhang B-W 2007 Phys. Rev. C **75** 051901 ; 2007 Int. J. Mod. Phys. E **16** 1930
[35] Wang X-N and Guo X 2001 Nucl. Phys. **A696** 788 ; Zhang B-W, Wang X-N, and Schäfer A, 2007 Nucl. Phys. A **783** 551; 2007 J. Phys. G **34** S809; Schafer A, Wang X-N and Zhang B-W 2007 Nucl. Phys. A **793** 128
[36] Harris B-W and Owens J-F 2002 Phys. Rev. D **65** 094032 Owens J-F 2002 Phys. Rev. D **65** 034011
[37] Zhang H-Z, Owens J-F, Wang E and Wang X-N 2001 Phys. Rev. Lett. **98** 212301; J. Phys. G 2007 **34** S801
[38] Owens J-F 1987 Rev. Mod. Phys. **59** 465
[39] Kunszt Z and Soper D-E 1992 Phys. Rev. D **46** 192
[40] Lai H-L *et al.* 2000 Eur.Phys.J. **C12** 375
[41] Albino S, Kniehl B-A and Kramer G 2008 Nucl. Phys. B**803** 42
[42] Bergmann L-J 1989 *Next-to-leading-log QCD calculation of symmetric dihadron production*, Ph.D. thesis, Florida State University
[43] Li S-Y and Wang X-N 2002 Phys. Lett. **B527** 85
[44] Wang E and Wang X-N 2001 Phys. Rev. Lett. **87** 142301; 2002 Phys. Rev. Lett.**89** 162301
[45] Wang E and Wang X-N 2001 Phys. Rev. C **64** 034901
[46] Florian D, Sassot R and Stratmann M 2007 Phys. Rev. D **75** 114010
[47] Adler S-S *et al.* (PHENIX Collaboration) 2006 Phys. Rev. Lett. **96** 202301
[48] Wang Q and Wang X-N 2005 Phys. Rev. C **71** 014903
[49] Straub P-B *et al* 1992 Phys. Rev. D **45** 3030
[50] Liu W and Fries R-J 2008 Phys. Rev. C **77** 054902
[51] Hwa R-C and Yang C-B 2003 Phys. Rev. C**67** 034902
[52] Greco V, Ko C-M and Levai P 2003 Phys. Rev. Lett.**90** 202302;
Phys. Rev. C**68** 034904
[53] Fries R-J, Muller B, Nonoka C and Bass S-A 2003 Phys. Rev. Lett.**90** 202303; Phys. Rev. C**68** 044902
[54] Hwa R-C and Yang C-B 2004 Phys. Rev. C**70** 024905
[55] Hwa R-C, arXiv:0904.2159
[56] Zhang H, Owens J-F, Wang E and Wang X-N 2007 Phys. Rev. Lett. **103** 032302
[57] Renk T 2006 Phys. Rev. C**74** 034906

[58] Bass S-A, Gale C, Majumder A, Nonaka C, Qin G-Y, Tenk T and Ruppert J 2009 Phys. Rev. C**79** 024901
[59] Gyulassy M, Vitev I, Wang X-N and Huovinen P 2002 Phys. Lett. **B526** 301
[60] Heinz U-W, arXiv:0901.4355 [nucl-th].
[61] Zapp K, Ingelman G, Rathsman J, Stachel J and Wiedemann U-A 2009 Eur. Phys. J. C**60** 617
[62] Renk T 2008 Phys. Rev. C**78** 034908
[63] Salgado C-A and Wiedemann U-A 2003 Phys. Rev. D**68** 014008
[64] Renk T and Eskola K 2007 Phys. Rev. C**76** 027901
[65] Gyulassy M, Levai P and Vitev I 2002 Phys. Lett. B **538** 282